

**Enhancing Li-ion conduction in composite polymer electrolyte by
 $\text{Li}_{0.33}\text{La}_{0.56}\text{TiO}_3$ nanotubes**

Lei Xu, Lifeng Zhang*, Yubing Hu, Langli Luo*

Institute of Molecular Plus, Tianjin University, 92 Weijin Road, Tianjin 300072,

P. R. China

*Corresponding authors. E-mail: lfzhang007@tju.edu.cn (L. Z.), [\(L.L.\).](mailto:luolangli@tju.edu.cn)

Experimental section

Synthesis of LLTO fillers

The LLTO NTs are fabricated by electrospinning method. A proportion of LiNO₃, LaNO₃·6H₂O, Ti(OC₄H₉)₄, and polyvinylpyrrolidone (PVP, M_w=1300000) are dissolved in dimethylformamide (DMF) and acetic acid solvent (volume ratio of DMF : acetic acid=4 : 1), and vigorous stirring for 24 h to form homogeneous solution. Then the solution is transferred into plastic capillary with a stainless-steel needle where the high voltage of 15 kV is applied. The grounded drum is placed at 15 cm away from the needle with a rotating speed of 300 r. p. m. The as-spun wires are annealed at 900 °C for 3 h with a heating rate of 10 °C·min⁻¹ in the tube furnace with argon atmosphere, then annealed at 900 °C for 6 h in a muffle furnace with a heating rate of 1 °C·min⁻¹ to form LLTO NTs. The LLTO nanowires (LLTO NWs) are fabricated by annealing at 900 °C for 3 h with a heating rate of 1 °C·min⁻¹ in the tube furnace with argon atmosphere and annealing at 900 °C for 6 h with a heating rate of 1 °C·min⁻¹ in muffle furnace. The LLTO nanoparticles (LLTO NPs) are prepared by sol-gel method. A certain proportion of LiNO₃, LaNO₃·6H₂O, Ti(OC₄H₉)₄, citric acid and ethylene glycol are dissolved in deionized water and stirred at 80 °C to form the sol. Then the sol was dried at 120 °C for 12 h and calcined at 900 °C for 6 h to form LLTO powders.

Fabrication of LLTO and PVDF composite polymer electrolytes

PVDF (M_w=500000) and LiClO₄ (weight ratio 2:1) are dissolved in DMF solution, then a proportion (5%, 10%, 15%, 20%, weight percentage) of LLTO NTs (or LLTO NWs, LLTO NPs) are added in the solution. The mixture is vigorously stirred for 24 h and

casted into polytetrafluoroethylene plate. Finally, the mixture is dried at 60 °C for 48 h at vacuum condition to form LLTO NTs and PVDF composite polymer electrolyte films (named 5% LLTO NTs CPE, 10% LLTO NTs CPE, 15% LLTO NTs CPE and 20% LLTO NTs CPE). The films filled with LLTO NWs and LLTO NPs are named LLTO NWs CPE and LLTO NPs CPE. The PVDF solid polymer electrolyte (PVDF SPE) is fabricated with above method without LLTO fillers. All the CPEs membranes are about 100 μ m in thickness.

Structure characterization of LLTO NTs CPEs

X-ray diffraction (XRD) tests of SSEs were characterized at Rigaku Smartlab9KW from 10° to 80° with a speed of 10°·min⁻¹. Scanning electron microscope (SEM) were tested at Thermo Scientific™ Apreo. Transmission electron microscope (TEM) characterization were carried at Thermo Scientific™ Talos F200X. Fourier transform infrared spectroscopy (FTIR) were characterized at Nicolet 6700. The solid-state nuclear magnetic resonance (SSNMR) were tested at JEOL JNM ECZ600R. Thermo gravimetric (TG) were carried at Netzsch TG 209F3 under N₂ atmosphere from 30-600 °C with a heating rate of 10 °C/min.

Electrochemical characterization of LLTO NTs CPEs

Electrochemical impedance spectroscopy (EIS) was characterized at Bio-logic SP200 with a frequency range from 7 MHz to 0.1 Hz. Linear sweep voltammetry (LSV) tests were conducted with Li|CPEs|stainless steel coin cells (CR2032) at a scanning rate of 1 mV·S⁻¹ at 25 °C. The coin cells (CR2032) of Li|CPEs|LiFePO₄ were assembled to test

the electrochemical properties of SSE. To fabricate LiFePO₄ cathode, LiFePO₄, PVDF and carbon black (weight ratio 8:1:1) were dissolved in NMP and stirred for 5 h, then casted on Al foils and vacuum dried at 60 °C for 12 h. The mass loading of LiFePO₄ was 1.1-1.2 mg·cm⁻².

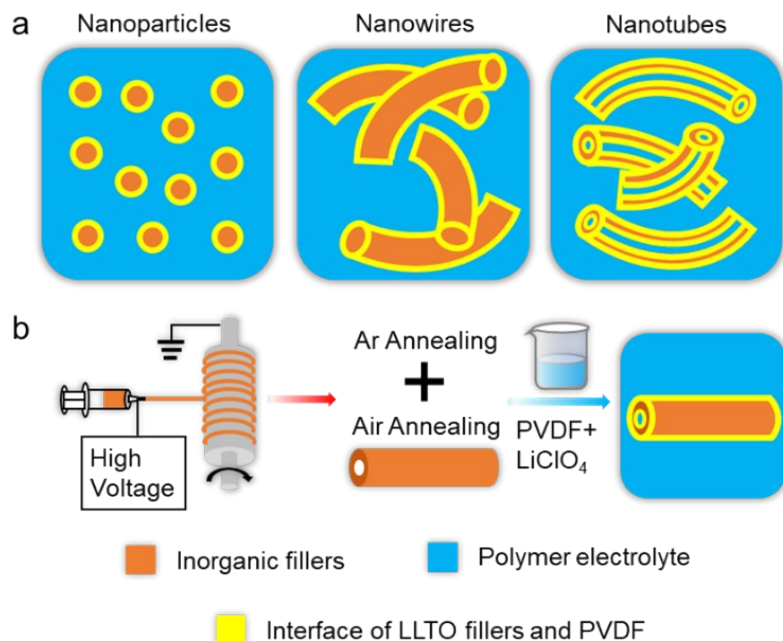


Fig. S1. Schematics of CPEs design and processing procedure. (a) The schematic of CPEs design with morphologically different inorganic fillers, highlighting their different interfaces with polymer matrix. (b) The schematic of processing procedure of nanotube fillers through an electrospinning method.

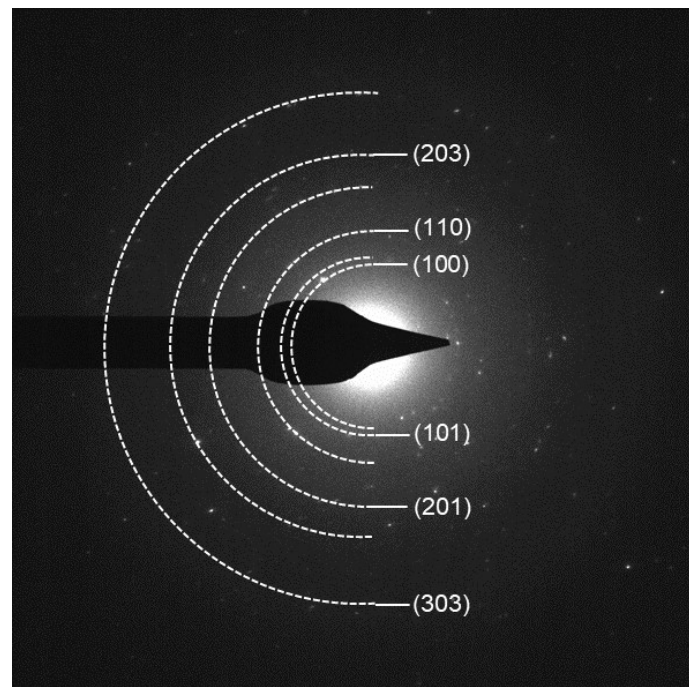


Fig. S2. SAED patten of LLTO NTs

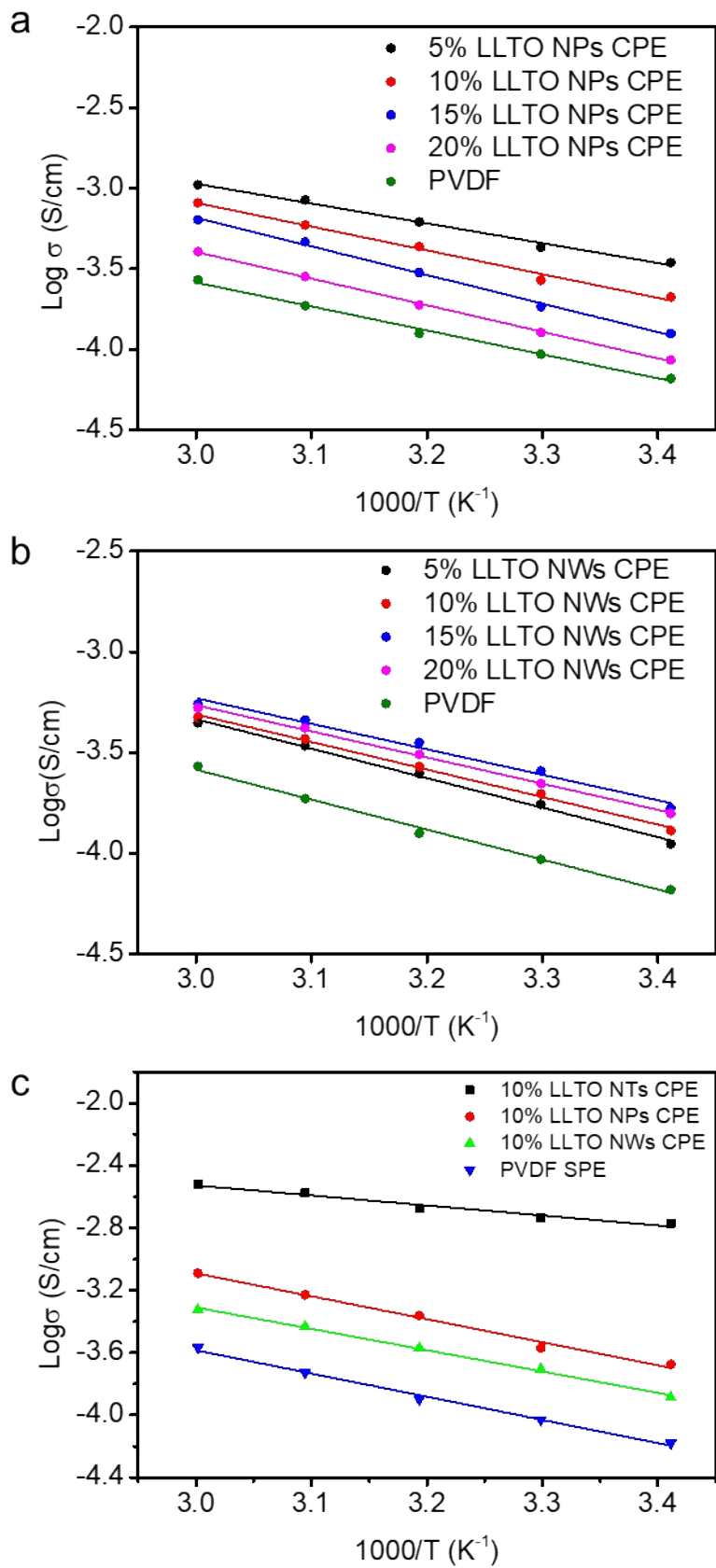


Fig. S3. Li-ion conductivity of CPEs with different LLTO NPs ratio (**a**) and LLTO NWs ratio (**b**).

Table. S1 The Li-ion conductivity of CPEs with various inorganic fillers and organic polymer.

Materials	Li-ion conductivity (S·cm ⁻¹)	Temperatur e (°C)	Ref
Li _{6.5} La _{2.5} Ba _{0.5} ZrTaO ₁₂ -PVDF CPE	3.4×10 ⁻⁴	20	1
Li _{6.4} La ₃ Zr ₂ Al _{0.2} O ₁₂ -PVDF CPE	1.5×10 ⁻⁴	25	2
Li _{6.4} La ₃ Zr _{1.4} Ta _{0.6} O ₁₂ -PVDF CPE	9.3×10 ⁻⁴	50	3
Li _{6.75} La ₃ Zr _{1.75} Ta _{0.25} O ₁₂ -PVDF CPE	5.0×10 ⁻⁴	25	4
Li ₇ La ₃ Zr ₂ O ₁₂ -PVDF-HFP CPE	9.5×10 ⁻⁴	25	5
Li _{6.5} La ₃ Zr _{1.5} Ta _{0.5} O ₁₂ -PVDF-HFP CPE	8.8×10 ⁻⁵	25	6
Li ₇ La ₃ Zr ₂ O ₁₂ -PVDF-HFP CPE	1.1×10 ⁻⁴	25	7
Li _{6.75} La ₃ Zr _{1.75} Ta _{0.25} O ₁₂ -PEO CPE	2.1×10 ⁻⁴	25	8
Li _{6.4} La ₃ Zr ₂ Al _{0.2} O ₁₂ -PEO CPE	2.5×10 ⁻⁴	25	9
Li _{6.4} La ₃ Zr _{1.4} Ta _{0.6} O ₁₂ -PEO CPE	1.6×10 ⁻⁴	30	10
Li ₇ La ₃ Zr ₂ O ₁₂ -PEO CPE	2.4×10 ⁻⁴	25	11
Li _{6.4} La ₃ Zr _{1.4} Ta _{0.6} O ₁₂ -PEO CPE	1.2×10 ⁻⁴	30	12
Li _{6.28} La ₃ Zr ₂ Al _{0.24} O ₁₂ -PEO CPE	8.5×10 ⁻⁵	25	13
Li _{6.75} La ₃ Zr _{1.75} Nb _{0.25} O ₁₂ -PMMA CPE	2.2×10 ⁻⁵	25	14
Li _{6.75} La ₃ Zr _{1.75} Ta _{0.25} O ₁₂ -PTFE CPE	1.2×10 ⁻⁴	25	15
Li _{0.33} La _{0.557} TiO ₃ -PEO CPE	2.4×10 ⁻⁴	25	16
Li _{0.35} La _{0.55} TiO ₃ -PEO CPE	8.8×10 ⁻⁵	25	17
Li _{0.35} La _{0.55} TiO ₃ -PVDF CPE	5.3×10 ⁻⁴	25	18
Li _{0.33} La _{0.557} TiO ₃ -PAN CPE	6.1×10 ⁻⁵	30	19
Li _{0.8} Sr _{0.2} Ga _{0.8} Mg _{0.2} O ₃ -PEO CPE	1.3×10 ⁻⁴	30	20
Li _{3/8} Sr _{7/16} Ta _{3/4} Zr _{1/4} O ₃ -PEO CPE	5.4×10 ⁻⁵	25	21
SiO ₂ -PEO CPE	6.0×10 ⁻⁴	30	22
Li _{1.4} Al _{0.4} Ti _{1.6} (PO ₄) ₃ -PVDF-PEO CPE	5.2×10 ⁻⁴	25	23
Li _{1.5} Al _{0.5} Ge _{1.5} (PO ₄) ₃ -PEO CPE	1.7×10 ⁻⁴	25	24
Li ₁₀ GeP ₂ S ₁₂ -CTMS-PEO	9.8×10 ⁻⁴	25	25
PETT-Ester -PVDF-HFP CPE	3.4×10 ⁻⁴	20	26
Li_{0.33}La_{0.56}TiO₃ nanotubes-PVDF CPE	1.7×10⁻³	20	This paper

Table. S2 The Li-ion conductivity and activation energy of CPEs with various morphologies LLTO fillers

Materials	Li-ion conductivity at 20°C (S·cm ⁻¹)	Activation energy (eV)
PVDF SPE	6.6×10^{-5}	0.30
5% LLTO NTs CPE	4.3×10^{-4}	0.20
10% LLTO NTs CPE	1.7×10^{-3}	0.13
15% LLTO NTs CPE	5.5×10^{-4}	0.24
20% LLTO NTs CPE	2.0×10^{-4}	0.29
5% LLTO NPs CPE	3.5×10^{-4}	0.24
10% LLTO NPs CPE	2.1×10^{-4}	0.29
15% LLTO NPs CPE	1.2×10^{-4}	0.35
20% LLTO NPs CPE	9.4×10^{-5}	0.33
5% LLTO NWs CPE	1.1×10^{-4}	0.29
10% LLTO NWs CPE	1.2×10^{-4}	0.27
15% LLTO NWs CPE	1.7×10^{-4}	0.25
20% LLTO NWs CPE	1.6×10^{-4}	0.26

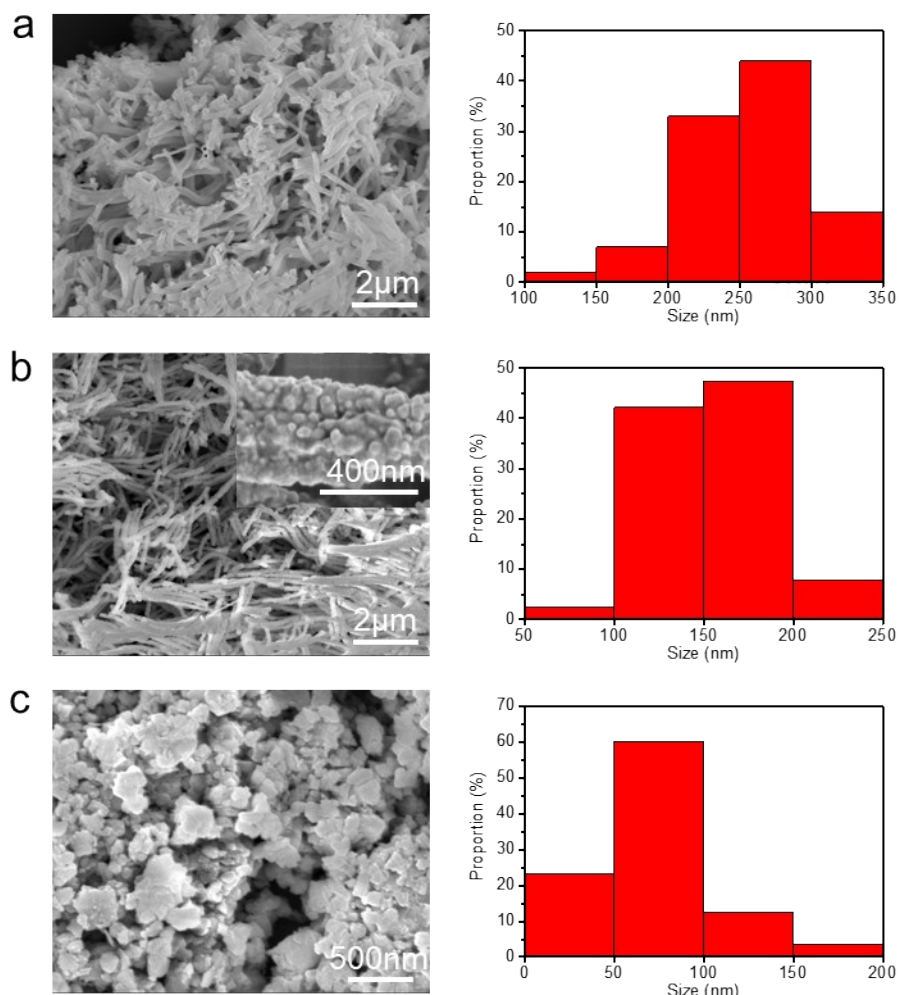


Fig. S4. SEM images of LLTO NTs (a), LLTO NWs (b) and LLTO NPs (c) with corresponding

size distribution.

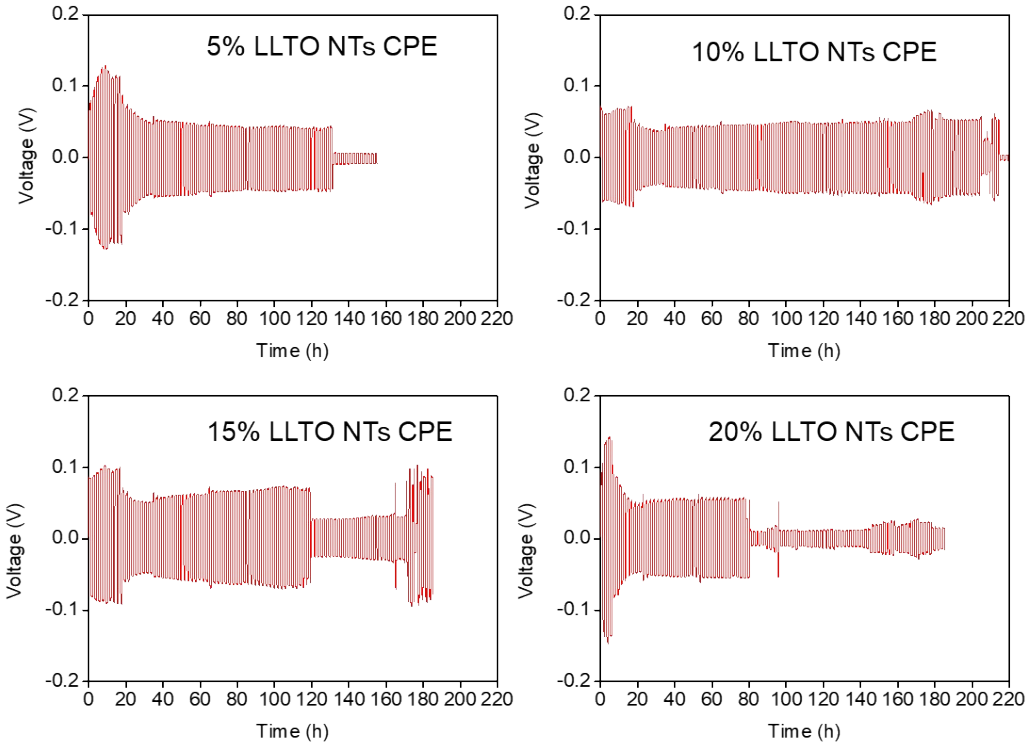


Fig. S5. Li|LLTO NTs CPEs|Li cells cycling performance with different LLTO NTs contents. The current density is $0.1\text{mA}/\text{cm}^2$, and the plating and stripping time are 1h respectively.

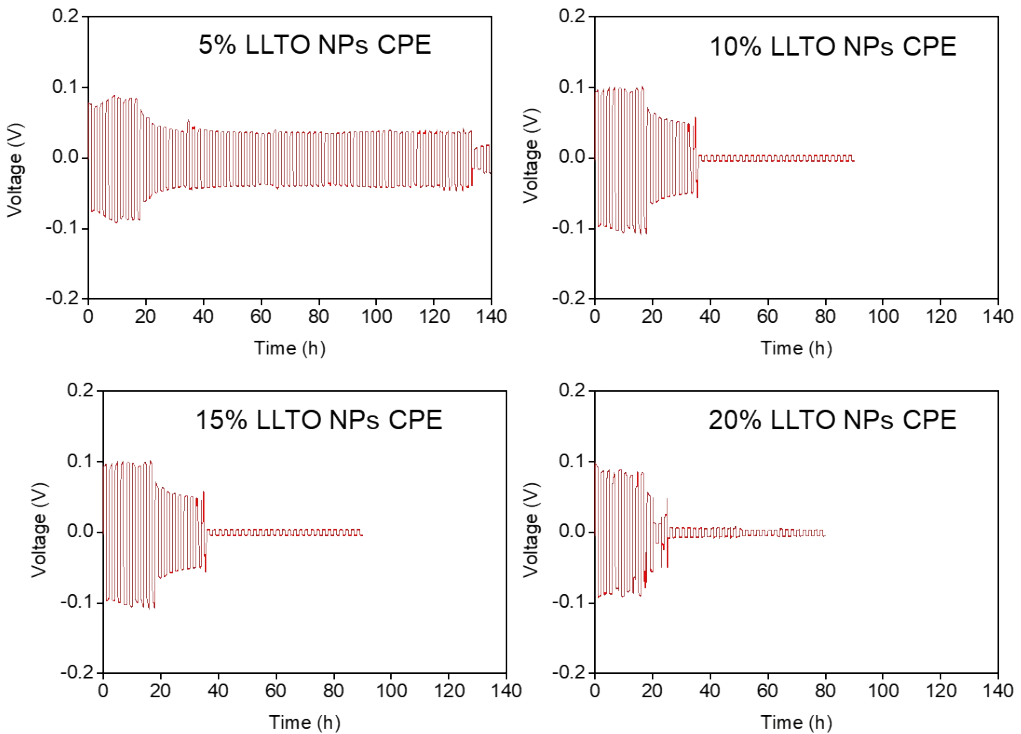


Fig. S6. Li-ion conductivity and Li|LLTO NPs CPEs|Li cells cycling performance with different LLTO NPs contents. The current density is $0.1\text{mA}/\text{cm}^2$, and the plating and stripping time are 1h

respectively.

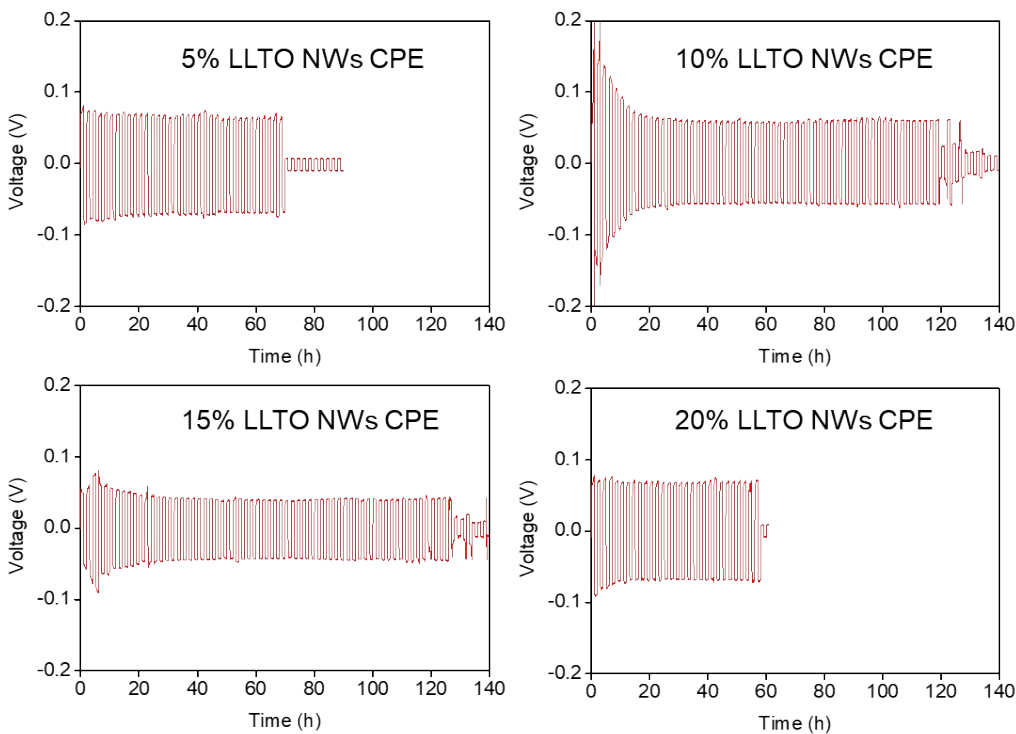


Fig. S7. Li-ion conductivity and Li|LLTO NWs CPEs|Li cells cycling performance with different LLTO NWs contents. The current density is $0.1\text{mA}/\text{cm}^2$, and the plating and stripping time are 1h respectively.

Reference

1. S. Bag, C. Zhou, P. J. Kim, V. G. Pol and V. Thangadurai, *Energy Storage Materials*, 2020, **24**, 198-207.
2. M. J. Wu, D. Liu, D. Y. Qu, Z. Z. Xie, J. S. Li, J. H. Lei and H. L. Tang, *Acs Applied Materials & Interfaces*, 2020, **12**, 52652-52659.
3. L. Gao, J. X. Li, J. G. Ju, B. W. Cheng, W. M. Kang and N. P. Deng, *Composites Science and Technology*, 2020, **200**, 9.
4. X. Zhang, T. Liu, S. F. Zhang, X. Huang, B. Q. Xu, Y. H. Lin, B. Xu, L. L. Li, C. W. Nan and Y. Shen, *Journal of the American Chemical Society*, 2017, **139**, 13779-13785.
5. Y. Li, W. Zhang, Q. Q. Dou, K. W. Wong and K. M. Ng, *Journal of Materials Chemistry A*, 2019, **7**, 3391-3398.
6. J. Lu, Y. C. Liu, P. H. Yao, Z. Y. Ding, Q. M. Tang, J. W. Wu, Z. R. Ye, K. Huang and X. J. Liu, *Chemical Engineering Journal*, 2019, **367**, 230-238.
7. W. Q. Zhang, J. H. Nie, F. Li, Z. L. Wang and C. Q. Sun, *Nano Energy*, 2018, **45**, 413-419.
8. R. Fan, C. Liu, K. Q. He, S. H. S. Cheng, D. Z. Chen, C. Z. Liao, R. K. Y. Li, J. N. Tang and Z. G. Lu, *Acs Applied Materials & Interfaces*, 2020, **12**, 7222-7231.
9. D. Cai, D. H. Wang, Y. J. Chen, S. Z. Zhang, X. L. Wang, X. H. Xia and J. P. Tu, *Chemical Engineering Journal*, 2020, **394**, 8.
10. H. Y. Huo, Y. Chen, J. Luo, X. F. Yang, X. X. Guo and X. L. Sun, *Advanced Energy Materials*,

-
- 2019, **9**, 8.
11. Z. P. Wan, D. N. Lei, W. Yang, C. Liu, K. Shi, X. G. Hao, L. Shen, W. Lv, B. H. Li, Q. H. Yang, F. Y. Kang and Y. B. He, *Advanced Functional Materials*, 2019, **29**, 10.
12. L. Chen, Y. T. Li, S. P. Li, L. Z. Fan, C. W. Nan and J. B. Goodenough, *Nano Energy*, 2018, **46**, 176-184.
13. J. Bae, Y. T. Li, F. Zhao, X. Y. Zhou, Y. Ding and G. H. Yu, *Energy Storage Materials*, 2018, **15**, 46-52.
14. J. Q. Sun, Y. G. Li, Q. H. Zhang, C. Y. Hou, Q. W. Shi and H. Z. Wang, *Chemical Engineering Journal*, 2019, **375**, 9.
15. T. L. Jiang, P. G. He, G. X. Wang, Y. Shen, C. W. Nan and L. Z. Fan, *Advanced Energy Materials*, 2020, **10**, 10.
16. P. Zhu, C. Y. Yan, M. Dirican, J. D. Zhu, J. Zang, R. K. Selvan, C. C. Chung, H. Jia, Y. Li, Y. Kiyak, N. Q. Wu and X. W. Zhang, *Journal of Materials Chemistry A*, 2018, **6**, 4279-4285.
17. J. Bae, Y. T. Li, J. Zhang, X. Y. Zhou, F. Zhao, Y. Shi, J. B. Goodenough and G. H. Yu, *Angew. Chem.-Int. Edit.*, 2018, **57**, 2096-2100.
18. B. Y. Li, Q. M. Su, L. T. Yu, D. Wang, S. K. Ding, M. Zhang, G. H. Du and B. S. Xu, *Acs Applied Materials & Interfaces*, 2019, **11**, 42206-42213.
19. W. Liu, S. W. Lee, D. C. Lin, F. F. Shi, S. Wang, A. D. Sendek and Y. Cui, *Nature Energy*, 2017, **2**, 7.
20. N. Wu, P. H. Chien, Y. M. Qian, Y. T. Li, H. H. Xu, N. S. Grundish, B. Y. Xu, H. B. Jin, Y. Y. Hu, G. H. Yu and J. B. Goodenough, *Angew. Chem.-Int. Edit.*, 2020, **59**, 4131-4137.
21. H. H. Xu, P. H. Chien, J. J. Shi, Y. T. Li, N. Wu, Y. Y. Liu, Y. Y. Hu and J. B. Goodenough, *Proc. Natl. Acad. Sci. U. S. A.*, 2019, **116**, 18815-18821.
22. D. C. Lin, P. Y. Yuen, Y. Y. Liu, W. Liu, N. Liu, R. H. Dauskardt and Y. Cui, *Advanced Materials*, 2018, **30**, 8.
23. S. H. Yi, T. H. Xu, L. Li, M. M. Gao, K. Du, H. L. Zhao and Y. Bai, *Solid State Ionics*, 2020, **355**, 10.
24. X. Wang, H. W. Zhai, B. Y. Qie, Q. Cheng, A. J. Li, J. Borovilas, B. Q. Xu, C. M. Shi, T. W. Jin, X. B. Liao, Y. B. Li, X. D. He, S. Y. Du, Y. K. Fu, M. Dontigny, K. Zaghib and Y. Yang, *Nano Energy*, 2019, **60**, 205-212.
25. K. C. Pan, L. Zhang, W. W. Qian, X. K. Wu, K. Dong, H. T. Zhang and S. J. Zhang, *Advanced Materials*, 2020, **32**, 8.
26. Y. Xia, Y. F. Liang, D. Xie, X. L. Wang, S. Z. Zhang, X. H. Xia, C. D. Gu and J. P. Tu, *Chemical Engineering Journal*, 2019, **358**, 1047-1053.